Gap Excitations and Series Loads in Microstrip Lines: Equivalent Network Characterization with Application to THz Circuits

Andrea Neto and Peter H. Siegel
Jet Propulsion Laboratory, California Institute of Technology

Abstract
At submillimeter wavelengths typical gap discontinuities in microstrip, CPW lines or at antenna terminals, which might contain diodes or active elements, cannot be viewed as simple quasi statically evaluated lumped elements. Planar Schotky diodes at 2.5 THz for example have a footprint that is comparable to a wavelength. Thus, apart from modelling the diodes themselves, the connection with their exciting elements (antennas or microstrip) gives rise to parasitics. Full wave or strictly numeric approaches can be used to account for these parasitics but at the expense of generality of the solution and the CPU time of the calculation. In this paper an equivalent network is derived that accurately accounts for large gap discontinuities (with respect to a wavelength) without suffering from the limitations of available numeric techniques.

I. INTRODUCTION

Planar circuits utilizing microstrip or coplanar waveguide are often coupled to active devices or antennas through electrically small gaps. However, at THz frequencies, practical fabrication scales limit devices, such as planar Schottky diodes [1], to dimensions which are comparable to a wavelength. As a consequence, the effect of the gap dimensions on the coupling coefficient or resonant frequency of the associated transmission line or antenna cannot be ignored. Nor can it be modelled as a quasi statically derived [2 and references there cited] single lumped element. In this paper the authors present a new formulation for analyzing the effect of finite gap excitations on microstrip lines. The technique involves separating the excited modes into reactive elements which are confined near to the gap and propagating quasi TEM components, which are coupled to the surrounding transmission line and load (antenna). The formulation is very general and can be applied to a large class of problems involving discontinuities in transmisssion line circuits. Verification of the new method has been obtained using traditional but much more time consuming method of moments (MoM) techniques [3, 4 for example].

Recent investigations [5, 6, 7] present a direct integration method to derive the spectral Green's function for microstrip and strip-line. Most notably they furnish a detailed analysis of the singularities of this Green's function, while enphasizing on the excitation mechanisms of the propagating and leaky modes compatible with strip line and microstrip. This technique can be used to great advantage in the modeling of sub-mm wave circuits. The same formalism was adopted by one of the authors, [8, 9] to derive, analytically in that case, the Green's function of a slot printed at the interface between two different homogeneous dielectrics, and in [10] to derive ad hoc basis functions in the MoM analysis of coplanar waveguide excited slot antennas.

As another application of this methodology, we investigate in this paper the input impedance of gap excited microstrips coupled to planar antennas. A rigorous equivalent network is derived that accurately accounts for the field in-and-near large-or-small (with

respect to a wavelength) gap discontinuities, without suffering from the lack of physical insight of purely numerically derived solutions. On the contrary the network approach will provide the guidelines on the one hand for the efficient coupling to and from the gap, and on the other hand for the separate characterization of the reactive energy associated with the feed. Full wave tools, such as Finite Difference in Time Domain or Finite Element Method may be necessary to characterize the minute details of a complicated diode structure but are typically not needed for the remaining part of the circuit.

In our technique the spectral kernel of the Greens function is first used for the determination of the bound mode wave number. Then the evaluation of the residue contributions associated with this pole allows the derivation of an equivalent transformer that accounts for the gap launching coefficient on the equivalent transmission line of the bound TEM mode in the microstrip. By subtracting the current associated with this main mode on the infinite line from the total current, a source attached current is defined. This current, for the circuit substrates used in many sub millimeter planar devices, is mostly confined in a region very close to the gap. From this current a parallel gap impedance is derived that accurately represents the reactive effects of the gap. The same formalism adopted here for the microstrip configuration, can be used for characterizing a wide variety of other gap excited planar transmission lines and active antennas.

II. FORMULATION: ELECTRIC CURRENTS ON THE MICROSTRIP

The problem under investigation is shown in Fig. 1.

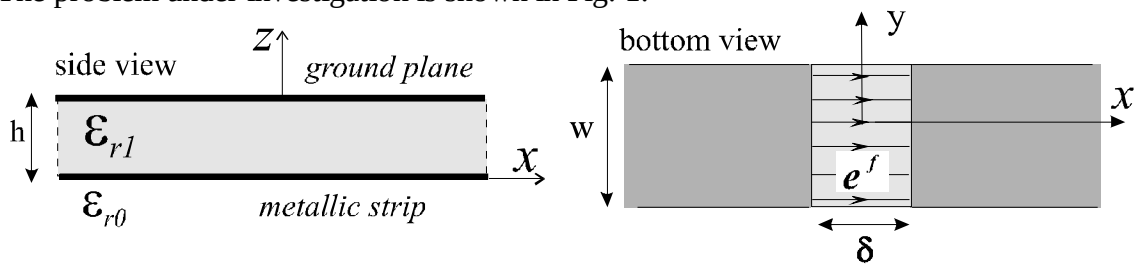

Fig.1 *Infinitely extended microstrip excited with by an impressed electric field distributed over a gap of dimensions (δ,w).*

An infinitely extended (along *x*) microstrip, printed on a grounded dielectric slab (ϵ_{r1}, $\epsilon_{r2}=1$) is considered. The microstrip cross section (*w*, along *y*) is uniform and much smaller than the wavelength. The structure is assumed to be excited by an impressed electric field $\boldsymbol{e_f}(x,y)=e_f(x,y)\boldsymbol{i}_x$. The electric current distribution is assumed to be characterized by a separable space-dependence with respect to *x* and *y*; i.e.,

$$j(x,y)=i(x)\cdot\frac{2}{w\pi}\frac{1}{\sqrt{1-\left(\frac{2y}{w}\right)^2}} \qquad (1)$$

where the transverse *y*-dependence is chosen to verify the quasi-static edge-singularities and the the normalization constant, $\frac{2}{w\pi}$, has been chosen in such a way that $i(x)$ represents a net current flowing in the microstrip at any cross section of the slot line. The method adopted to derive the current of a gap excited microstrip has been presented in [5]-[7]. A

brief review with the minor variations introduced in this paper is presented in the appendix. As a result the electric current in the microstrip is expressed as:

$$i(x)= \frac{1}{2\pi} \int_{-\infty}^{\infty} \frac{-E^f(k_x)e^{-jk_x x}}{D(k_x)} dk_x \qquad (2)$$

where $E^f(k_x)$ is the Fourier Transform (FT) of the impressed electric field, with respect to the variable x, and

$$D(k_x)= \frac{1}{2\pi} \int_{-\infty}^{\infty} G_{xx}(k_x,k_y)J_0(\tfrac{1}{2}w_s k_y)dk_y \qquad (3)$$

with J_0 is the Bessel function of zero order and $G_{xx}(k_x, ky)$ the FT, with respect to the variables x and y of the electric field radiated by a short electric dipole lying at the interface between the slab and the homogeneous half space for $z<0$, in the absence of the metallic strip.

An interesting aspect of (2) is that the impact of the feed is all contained in the numerator and in most practical cases it is a simple anayitic function. When the distribution is uniform over the feed region $e^f(x)=-1/\delta$ for $x \in (-\delta/2,\delta/2)$ the excitation is said to be a δ-gap and $E^f(k_x)= -sinc(k_x\delta/2)$. This case will be considered specifically in the following. The denominator, $\frac{1}{D(k_x)}$, represents the microstrip spectral Green's function and for a detailed discussion on the nature of the branch singularities of $D(k_x)$ the reader is referred to [5, 6].

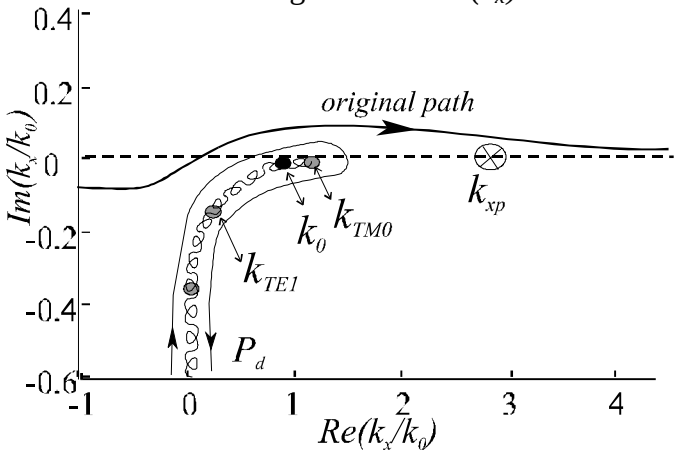

Fig. 2 *Complex k_x plane topology for thin dielectric substrates. Only the TM0 pole of the grounded slab is assumed to be above cut off.*

The outer integral in (2) can be performed by adopting a deformation in the complex plane below the real axis for Re $(k_x)<0$ and above the real axis for Re $(k_x)>0$ (*original path* in Fig. 2), in order to avoid the branch cuts arising from the branch points implicit in $D(k_x)$. Here it is sufficient to know that these branches are square root type or logarithmic when they originate from poles or from the branch (k_0) of the layered Green's function $G_{xx}^{je}(k_x,k_y)$ respectively. For a thin dielectric layer configuration, (that is only the TM0 pole

is above cut off in the grounded slab) the complex plane topology of the microstrip's Green's function, $\frac{1}{D(k_x)}$, is well represented in *Fig. 2* which shows the branch cuts arising from k_{TM0}, k_{TE1} and k_0.

II.1 Case study

It is instructive to perform a parametric study of the currents as a function of the gap dimensions. The information derived will lead to the current representation and equivalent network of the following sections. Fig. 3. shows the real part (3a) and imaginary part (3b) of the current due to a 1 volt uniform excitation for different gap dimensions (δ) from 2 to 18 μm. The width of the microstrip (w) and the height of the slab (h) are 8 μm and 3 μm respectively ($h=\lambda_0/40$ *at 2.5 THz*). The relative dielectric constant considered is ϵ_{r1}=12.85. These parameters and the maximum gap dimension are typical of thin GaAs membrane diode technology [1] for which this analysis is derived.

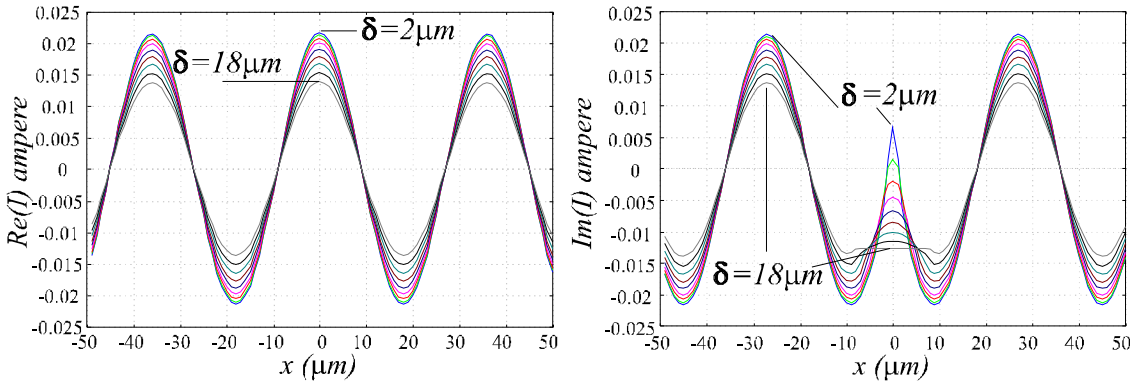

a) b)

Fig. 3 *Current on an example microstrip structure at submillimeter wave frequencies (2.5 THz) obtained using the present direct integration method (equation 2). Real (a) and Imaginary(b) parts are presented for different dimensions of the excitation gap (δ varying from 2 to 18 μm).*

Two aspects of the problem should be noted

i) A launching efficiency issue stands out, since the amplitude of the oscillation of the real and imaginary part of the current at a certain distance from the source is regulated by the gap dimensions. As δ tends to zero, the amplitude of the current is a maximum and tends to one half of the characteristic admittance of the microstrip line. As δ grows the value of the current diminishes.

ii) The reactive energy in the feed zone is strongly affected by the width of the source. When the gap dimensions shrink to zero, the imaginary part of the current tends to grow logarithmically (Fig. 3b) indicating a capacitive reactance. When the dimensions of the gap are large, the imaginary part of the current can be less then zero, indicating an inductive reactance.

II.2 Modal and source attached currents

The dispersion equation, $D(k_x)=0$, defines the position of the pole of the guiding structure. The localization of the zeroes of $D(k_x)$ as a function of the parameters of the structure (w, ϵ_{r1}), can be performed numerically by means of a descent along the gradient algorithm. As

a starting point one can use the analytical formulas [1], knowing that the actual propagation constant is not drastically different. Only one pole, indicated here after as $\pm k_{xp}$, is found for the thin dielectric layers we are interested in ($3\mu m = \frac{\lambda_0}{40}$ *at 2.5 THz*). In the absence of losses, the pole of the structure is found on the real axis of the k_x plane (see *Fig. 2*). Knowingn its location, the integral in *(2)* can be approximated asymptotically for $|x| > \delta/2$, by the residues of the poles in $k_x = \pm k_{xp}$. These residue contributions are expressed as

$$i_{res}(x) = -2\pi j\left(sinc\,(k_{x0}\tfrac{\delta}{2})\right) R\, e^{-jk_{xp}|x|} R = Res\left(\frac{1}{D(k_x)}\right)_{k_x = k_{xp}} \qquad (4)$$

It is apparent that this current is the one associated with the quasi TEM mode that propagates in the microstrip. A comparison between the residue evaluation *(4)* of the integral in *(2)* and the original numerical integration is presented in Fig.4a and Fig. 4b, for two unit δ-gap excitation configurations. Outside the source region (gray zone in Fig. 4) the full integration of *(2)* and the sole residue contribution are almost superimposed due to the drawing scale. A source attached current can then be defined and will be indicated by

$$i^s(x) = i(x) - i_{res}(x) \qquad (5)$$

The source attached currents represent an overall current that contains all the separate branch conntributions, without calculating them separately as in [7]. In this respect it is useful to observe that i^s can be calculated for $|x| > \delta/2$, deforming the original integration path on a path P_d (Fig. 2 where only the spectrum for $\mathrm{Re}(k_x) > 0$ is shown) that surrounds all the branch cuts on the top Rieman sheet. This is possible because in thin dielectric cases, the only significant singularity encountered in the deformation is the pole in $\pm k_{xp}$.

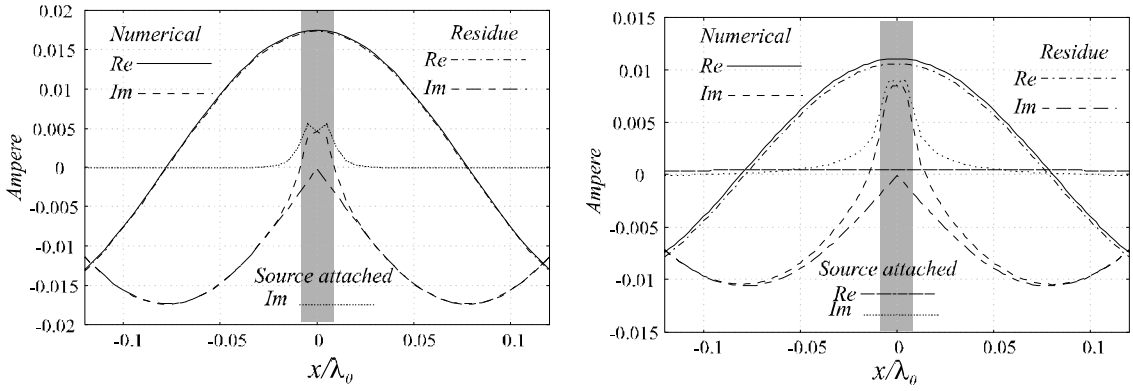

a) b)

Fig. 4 *Comparison between asymptotic evaluation (residue only) and direct numerical integration of the current for a sample microstrip structure at submillimeter wave frequencies (2.5 THz). Also plotted is the source attached field (real and imaginary parts in 4.b and only the imaginary part in 4.a since the real part is almost zero and cannot be distinguished in the drawing scale). The width of the microstrip and the dimensions of the excitation gap (δ) are $\lambda_0/20$ ($6\mu m$), $\lambda_0/60$ ($2\mu m$) respectively. The height of the slab is $\lambda_0/40$ ($3\mu m$) in Fig. 4a and $\lambda_0/20$ ($6\mu m$) in Fig. 4b. The relative dielectric constant considered is ($\epsilon_{r1}=12.85$).*

The integrand decays exponentially in the deformed path P_d. Thus the numerical calculation of i^s is much more efficient than along the original path. The definition of the source attached current is also analytically extended to the source region, $|x| < \delta/2$ (but not this way of calculating it, which must be done in accordance with the definition in *(5)*). The source attached field is also plotted in Fig. 4. In [7] it is demonstrated that each of the branch contributions to the current decays as $x^{-3/2}$, thus also $i^s(x)$ decays this way or faster. It's value in the source zone depends on the thickness of the dielectric considered. In the very thin dielectric slab ($h=\lambda_0/40$) considered in Fig. 4a the real part of $i^s(x)$ is not noticeable on the drawing scale and thus is not reported. Also the imaginary part of $i^s(x)$ is very concentrated in the surrounding of the source. In Fig. 4b the same curves are reported for a thicker dielectric case ($h=\lambda_0/20$). In this case the real part of $i^s(x)$ is noticeable, and significant for larger distances from the source. It is worth repeating at this point that ($h=\lambda_0/40$) corresponds to a 3μm thick dielectric at 2.5 THz, the design target for this work.

III. INPUT ADMITTANCE AND EQUIVALENT NETWORK

The current representation in terms of source attached and mode contributions is particularly significant when only one bound mode is propagating in the microstrip. In this case it is possible to derive a rigorous equivalent network, based on a single transmission line, that characterizes the δ-gap excited infinite microstrip input impedance. We will see in section IV, that finite (loaded) microstrips can also be studied by resorting to the same simple equivalent network. The input admittance of a δ-gap excited microstrip can be expressed in the spectral domain as:

$$y_{inf} = \int_{-\infty}^{\infty} \frac{sinc^2(k_x\delta/2)}{D(k_x)} \, dk_x \qquad (6)$$

Accordingly, the total complex power radiated by the source can be expressed as:

$$P_{tot} = \tfrac{1}{2} \, | V_g | ^2 y_{inf} \qquad (7)$$

The knowledge of the microstrip characteristic impedance z_0 [3], together with the amplitude of the traveling wave in the microstrip from *(4)*, consents to write the power launched in the microstrip quasi TEM mode as:

$$P_m = | V_g | ^2 (R^+)^2 z_0 \qquad (8)$$

where $R^+ = -2\pi j \left(sinc\,(k_{x0}\tfrac{\delta}{2}) \right) R$. This power actually leaves the excitation zone in form of a couple of outgoing travelling waves ($\pm k_{xp}$). As we will see later on, this power is the only one that might give rise to interactions with components of the circuit which are located at a significant distance, in terms of a wavelength, from the feeding zone. In order to derive an equivalent network that rigorously takes into account the gap effects one may associate all the power that is not launched into the the quasi TEM mode as being assigned to a lumped load indicated as z_{gap}. The power conservation then imposes:

$$P_{gap} = P_{tot} - P_m \qquad (9)$$

This gap impedance is imagined as in parallel to the source and to the modal loading as in fig. 5a. Accordingly both P_m and P_{gap} can also be expressed as:

$$P_m = \tfrac{1}{2} \mid V_g \mid^2 y_m; \qquad P_{gap} = \tfrac{1}{2} \mid V_g \mid^2 y_{gap} \tag{10}$$

thus givin the explicit relation between the various admittance components of the network in fig.5a

$$y_{gap} = y_{inf} - y_m \tag{11}$$

The expression for y_m according to this definition equating the two expression for P_m in *(8)* and *(10)*

$$y_m = 2(R^+)^2 z_0 \tag{12}$$

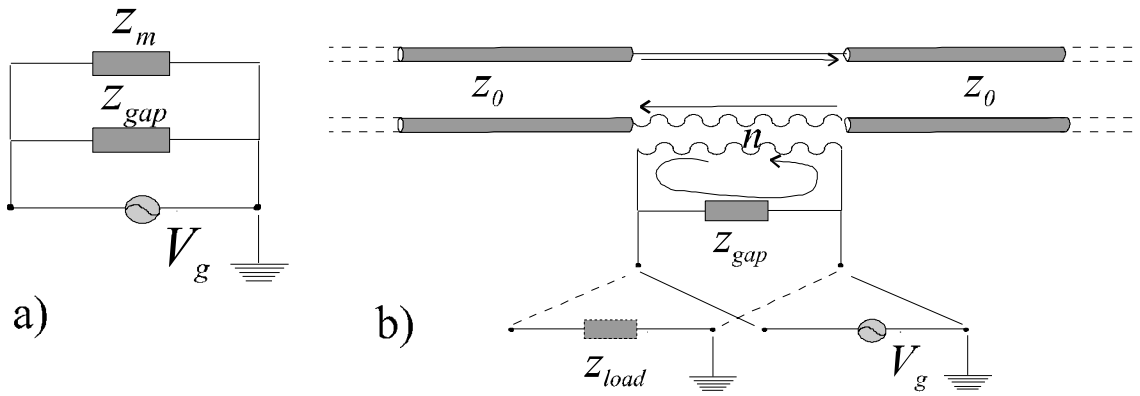

Fig. 5 *Equivalent network for δ gap excited microstrip structure. a) admittance decomposition ($y_{inf} = y_{gap} + y_m$); b)Interpretation of the modal impedance interms of transformer connected equivalent transmission line.*

So that, given *(12)*, *(11)* becomes an operative definition. It is useful to perform a further algebraic manipulation expressing the modal admittance as

$$y_m = \frac{2z_0 R^+ \cdot 2z_0 R^+}{2z_0} = n^2 \frac{y_0}{2} \tag{13}$$

where

$$n = 2z_0 R^+ = 2z_0 (2\pi j R)\ sinc\ (k_{x0} \tfrac{\delta}{2}) \tag{14}$$

The introduction of the coefficient *n* consents to represent the modal part of the impedance associated to the series of two transmission lines representing the quasi TEM mode. These transmission line are series fed, via a transformer of turn ratio *n*, by the parallel combination of the source voltage and the gap impedance. The full circuit is shown in Fig. 5b.

The use of the transformer is a convenient wayof separating the different field behavior associated with the feeding and the propagation of the transmission lines. The electric currents in the source are oriented parallel those in the microstrip, both along x. The electric fields in the source and in the transmission line are orthogonal, (along x and along

z respectively). The value of the transformer *n* for the same microstrip of Fig.3 (operated again at 2.5 THz) is plotted in Fig. 6. as a function of the gap's width, δ.

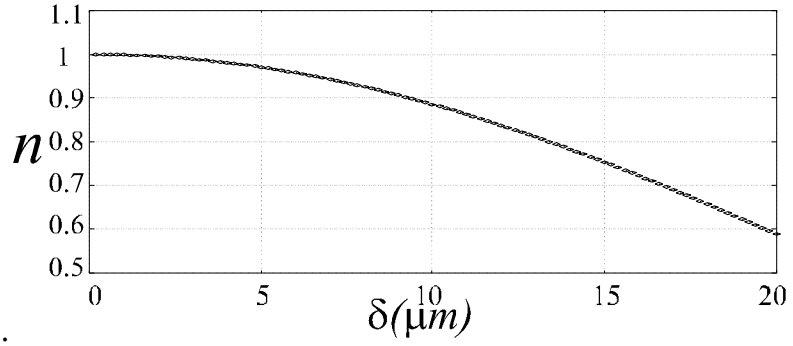

Fig. 6 *Transformer for δ gap excited microstrip structure of Fig. 3*

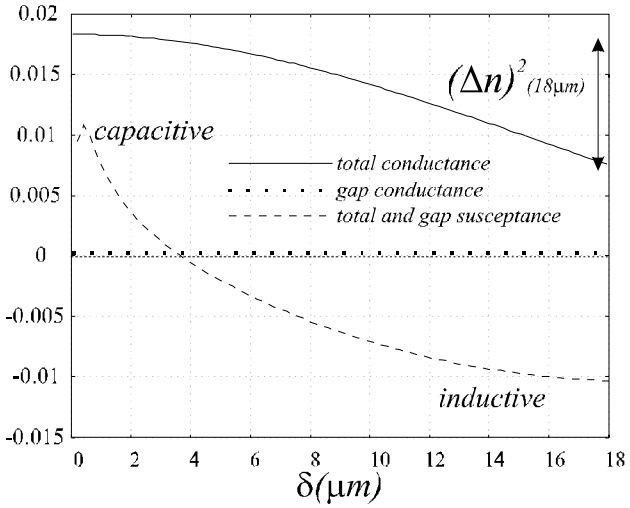

Fig. 7 *Total and gap admittance (gap and total susceptances are equal)*

The gap and total admittance for to the same case are presented in *fig.7*. It should be noted that the gap conductance is virtually zero for the case of the thin dielectric slab, and the gap susceptance, coincident by definition with the total one, goes from being capacitive to inductive for the investigated range of δ.

IV. NUMERICAL EXAMPLES, APPLICABILITY AND CONSIDERATIONS

The purpose of deriving the equivalent network is to characterize the input impedance of finite, as opposed to infinite, microstrips. When the bound mode currents are much more intense than the source attached currents, at a certain distance from the source one may assume that the source attached currents intrinsically satisfy Maxwell's equations for the finite structure. The loading of the end-points of the microstrip will generate a reflection that can be characterized by a load impedance. Thus the interaction between the two outer loads and the source can be accounted for via a complete equivalent network with equivalent lumped elements z_{l1}, z_{l2} (Fig. 8) located at the endpoints of the microstrip.

IV.1 Numerical examples

Two finite length microstrips printed on a GaAs membrane ($\epsilon_{r1}=12.85$) have been investigated using the equivalent network in fig. 8.

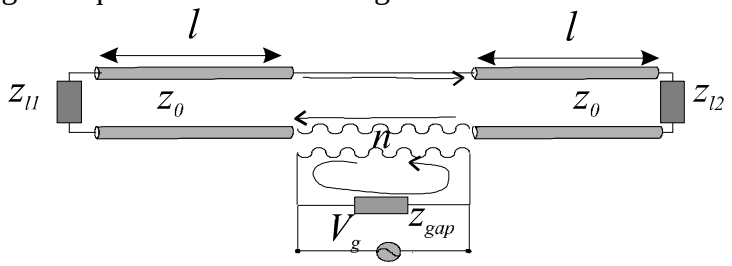

Fig.8 *Equivalent network for a δ-gap excited and loaded microstrip.*

The dielectric thicness and the width of the conductor are 3 μm and 2.5 μm respectively. The pertinent open end impedance has been derived as in [3]. Fig.9a shows the imaginary part of the input impedance for a 60μm long microstrip as a function of the frequency for three different gap dimensions (0.5, 1.15, and 15 μm). It is found that in the three cases the resonant frequency is the same and significant differences are observed at larger values of the impedance. Also the pertinent curves obtained via a full wave Method of Moments are shown for the 1.15 μm and the 15 μm cases. The MoM tool uses piece wise sinusoidal sub-domain basis functions and rectangular weighting functions in the longitidinal dimension and assumes a rectangular distribution in the transverse dimension. The agreement between the network solution and the MoM solution is excellent apart for a minimal (0.5 %) resonant frequency shift, probably due to the different electric current transverse distribution assumed in the two models.

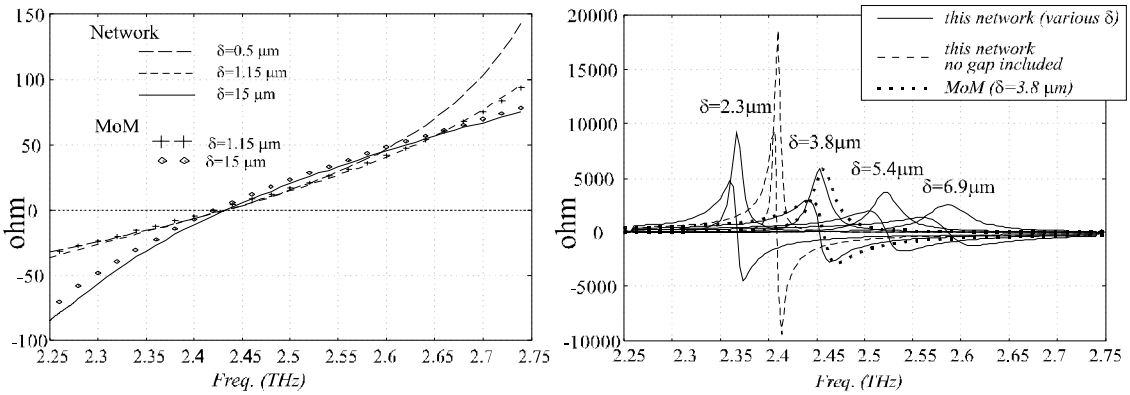

a) b)

Fig. 9 *Impedance of a delta gap excited microstrip as function of the frequency. a) (l=60 μm); b) l=40μm). Also a parametric study as a function of δ and comparison with MoM are shown. The width of the microstrip and the thickness of the dielectric are 2.5 μm and 3 μm respectively. The grounded dielectric is made of Ga-As.*

The case in Fig. 9a ($l=60\ \mu m$) is geometry corresponds to a case in which the load impedance (z_{li}, $i=1,2$), when reflected the excitation zone, is nearly zero. In view of this the gap impedance effect is relatively minimal since it is in parallel to a very low impedance load. The case in Fig. 9b ($l=40\mu m$) corresponds to a very high load impedance

at the excitation zone, and as seen the impact of the gap becomes dramatic. The resonant frequency as a function of the gap width shifts very significantly for δ varying from 2.3 μm to 6.9 μm and the curves can easily be distinguished. For even smaller gaps the resonance frequency shifts out of the figure since the source attached currents tend to be singular as δ tends to zero. In Fig.9a is also plotted a MoM result, for δ=3.84 μm, which again shows excellent agreement with out model. Finally in Fig. 9b the result that would be achieved by using the equivalent network without the transformer and the gap impedance introduced in this paper is plotted. Not only is the resonance frequency poorly modelled but also the absolute values of the impedance vary widely form those of the more accurate equivalent network analysis.

IV.2 Applicability

We will assume than when $|\, i_s(x=l/2)\,| < \frac{|i_{res}(x=l/2)|}{100}$ the accuracy, $A(x=l/2) > \frac{1}{100}$, in the evaluation of input admittance is satisfactory. In fig. 10 $|\, i_{res}\,| / |\, i_s\,|$ is plotted as a function of the frequency at an observation point located at $\lambda_0/10$ from the center of the feed. The microstrip's nominal characteristic impedance is 50 ohms, the dielectric thickness and the width of the conductor strip are 3 μm and 2.5 μm respectively. The dimension of the excited gap is $\lambda_0/40$ and the dielectric is composed of silicon ($\epsilon_{r1}=11.7$). It is found that $|\, i_{res}\,| / |\, i_s\,|$ is always larger than 100 for frequencies up to 3 THz. Thus, since $i_s(x)$ decays algebraically, $x^{-3/2}$, any load at a distance larger than $\lambda_0/10$ can be characterized accurately with the present equivalent network. The same is not true for thicker dielectrics. Also the investigated microstrip is only weakly dispersive, as the normalized propagation constant k_{xp}/k_0 calculated as explained in sect. III varies from *2.8 to 2.9* in the frequency range considered in *Fig. 10.*

IV.3 Considerations

The loads, Fig. (8), typically represent active impedances. For example if they represented slot antennas their impedance should be calculated when both slots are radiating in phase. In this case the load connected at the end points of the microstrip will present a larger real part. Also in this case frequency shifts as significant as in Fig. 9b, can be expected. This has already been experimentally verified in a similar slot circuit [11]. If the actual source under investigation is not well represented by a δ-gap generator, a correction in the equivalent network parameters can be made by simply substituting the *sinc* function in *(6), (14)* with the relevant FT $E^f(k_x)$, provided the more realistic function $e^f(x)$ is still an even function, with respect to x. If $e^f(x)$ also presents some odd components, then a single impedance should not be used, and an even and odd impedance characterization should be adopted. The extra degree of freedom (odd mode) can still benefit from an equivalent network, that can be derived with the same methodology used here for the even mode. At this point $e^f(x)$ could for example the result of the investigation of complicated source in isolation. Indeed the procedures presented in this paper are found to be particularly useful in connecting an isolated load or source to the remaining part of the circuit. Full wave tools such as Finite Difference Time Domain or Finite Element Method may be necessary to caharacterize the tiny details of a complicated source (like a diode) but are often not necessary for analyzing the remaining part of the circuit.

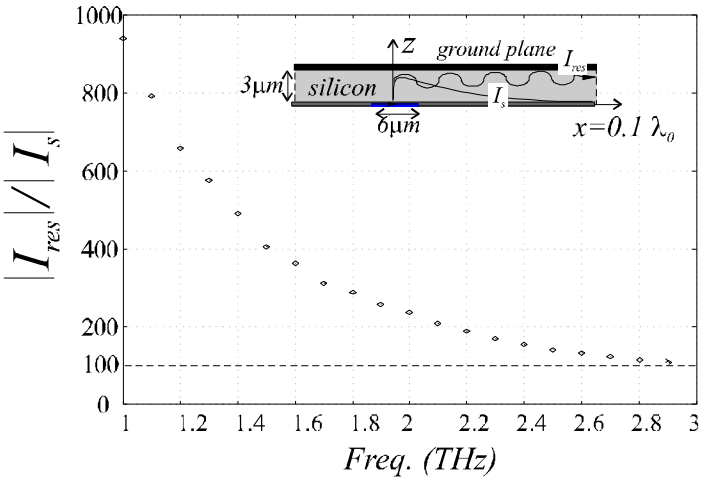

Fig. *10 Ratio between the amplitudes of the residue contribution to the currents and the source attached currents. The graph can be read as 1/(A(l=0.1λ$_0$)). The microstrip impedance is nominally 50 ohm. The width of the microstrip and the thickness of the dielectric are 2.5 μm and 3 μm respectively. The grounded dielectric is made of silicon (ϵ_{r1}=11.7). The width of the gap is λ$_0$/40.*

V. CONCLUSIONS

An equivalent network has been presented for the wide band characterization of the gap in a series fed and loaded microstrip line. The network consists of a transformer and a gap impedance. The transformer accounts for the launching coefficient of the mode on the equivalent transmission line representing the microstrip and is evaluated analytically by simple interpretation of the spectral expression of the microstrip Green's function. The gap impedance accounts for the current distribution in the region surrounding the feed, and is calculated by simple spectral domain numeric integration (less then 3 minutes on a 300 MHz Pentium II). The procedure, validated via MoM, will work for any kind of dielectric stratification, but is meaningful when one bound mode is above cut off in the microstrip. Submillimeter's wave problems in which this equivalent network can be applied include the design of receivers (i.e. diodes as mixers or frequency multipliers) and generators (i.e. photomixer based local oscillators).

APPENDIX: SOLUTION OF THE INTEGRAL EQUATION

According to the equivalence principle an Electric Field Integral Equation (EFIE) is set up and enforced, via a point matching like procedure only on the longitudinal axis of the micro strip *(y=0)*.

$$\iint_{\Sigma} g_{xx}(x-x', 0-y')\, j_x(x', y')\, dx'dy' = -e^f(x, 0) \qquad (A0)$$

where Σ is the entire microstrip domain. The point matching (or razor blade) as testing procedure is selected in order to mantain the same formalism used [8-10] for the characterization of slot antennas printed between two different homogeneous dielectrics. All the quantities are scalar, because of the x-polarisation of all the scattered and impressed electric fields involved in the equation, and neglecting cross polarized electric

currents (in view of the small cross section of the strip). The left hand side of *(A0)* represents the electric field at $z=0$ radiated by the electric current density j_x. The Green's function, g_{xx}, that appears in the kernel of this integral equation, is the electric field radiated by a short electric dipole lying at the interface between the slab and the homogeneous half space for $z<0$, in the absence of the metallic strip.
The electric current distribution is assumed to be characterized by a separable space-dependence with respect to x and y; i.e.,

$$j(x',y')=i(x') \cdot j_t(y') \,. \qquad (A1)$$

The transverse y-dependence is chosen to verify the quasi-static edge-singularities

$$j_t(y)=\frac{2}{w\pi}\frac{1}{\sqrt{1-\left(\frac{2y}{w}\right)^2}}. \qquad (A2)$$

$j_t(y)$ possesses a closed-form Fourier transform,

$$J_t(k_y)=FT\{j_t(y)\}=J_0(\tfrac{1}{2}w\,k_y), \qquad (A3)$$

where J_o is the Bessel function of zero order. The IE (1) is now transformed into the k_x-Fourier domain as

$$I(k_x)\int_{-\infty}^{\infty}\widetilde{G}_{xx}(k_x,\ -y')\ j_t(y')\,dy' = -E^f(k_x), \qquad (A4)$$

where $I(k_x)$ and $\widetilde{G}_{xx}(k_x, -y')$ are the FT, with respect to the variable x, of $i(x)$ and $g_{xx}(x, y)$, respectively. Equating the two spectra in k_x it is apparent that

$$I(k_x)=\frac{-E^f(k_x)}{D(k_x)}; \qquad (A5)$$

where

$$D(k_x)=\int_{-\infty}^{\infty}\widetilde{G}\,(k_x,\ -y')\ j_t(y')\,dy'=\frac{1}{2\pi}\int_{-\infty}^{\infty}G(k_x,k_y)J_0(\tfrac{1}{2}w_s k_y\,)dk_y \qquad (A6)$$

represent the spectral domain Green's function of the microstrip line and $G(k_x,k_y)$ is the FT of $g(x, y)$ with respect to both the variables x and y. The electric current on the microstrip can then be expressed as:

$$i(x)=\frac{1}{2\pi}\int_{-\infty}^{\infty}\frac{-E^f(k_x)e^{-jk_x x}}{D(k_x)}\,dk_x \qquad (A7)$$

References

[1] P.H. Siegel, R. P. Smith, M. C. Gaidis, S. Martin "2.5 THz GaAs Monolithic Membrane-Diode Mixer," *IEEE Trans. Microwave Theory and Techniques, vol. MTT 47*, pp. 596-604, May 1999.

[2] P. Benedek, P. Sylvester, " Equivalent Capacitance for Microstrip Gap and Steps," *IEEE Trans. Microwave Theory and Techniques*, vol. MTT 20, pp. 729-733, Nov. 1972.

[3] P.B. Katehi, N.G. Alexopoulos, "Frequency Dependent Characteristics of Microstrip Discontinuities in mm-Wave Integrated Circuits," *IEEE Trans. Microwave Theory & Techniques.*, vol. MTT 33, no. 10, pp. 1029-35, Oct. 1985.

[4] N.G. Alexopoulos, Shih-Chang Wu "Frequency Independent Equivalent Circuit Model for Microstrip Open-End and Gap Discontinuities," *IEEE Trans. Microwave Theory & Techniques.*, vol. MTT 42, no. 7, pp. 1268-1272, July 1994.

[5] C. Di Nallo, F. Mesa, D.R. Jackson. "Excitation of Leaky Modes on Multilayer Stripline Structure" on *IEEE Transactions on Microwave Theory and Techniques,* Vol. 46, no. 8 , pp 1062 -1071, August 1998.

[6] F. Mesa, C. Di Nallo, D.R. Jackson "The theory of surface-wave and space-wave leaky-mode excitation on microstrip lines" on *IEEE Transactions on Microwave Theory and Techniques,* Vol. 47, no. 2 , pp. 207 -215, Feb. 1999.

[7] D.R. Jackson, F. Mesa, M.J. Freire, D.P. Nyquist, C. Di Nallo, "An Excitation Theory for Bound Modes and Residual-Wave Currents on Stripline Structures" *Radio Science*, Vol. 35, no. 2, pp 495 -510, March-April 2000.

[8] A. Neto, S. Maci, "Analytical Solution for Gap-Excited, Infinite Printed Slot Lines", to be presented at *IEEE Antennas and Propagation Symposium,* Boston July, 2001.

[9] A. Neto, S. Maci, "Green's Function of Gap-Excited, Infinite Printed Slot Lines", *NASA New Technology Report* (April 2001).

[10] A. Neto, P.J.I. De Maagt, S. Maci "Optimized Basis Functions for Slot Anetnnas Excited by Coplanar Waveguides", submitted to *IEEE Trans. Antennas and Propagation* (March 2001)

[11] R.A. Wyss, A. Neto, W.R. McGrath, B. Bumble, and H. LeDuc, "Submillimeter-wave spectral response of twin-slot antennas coupled to hot electron bolometers," Proceedings of the *11-th Int. Symp. on Space THz Tech.*, Ann Arbor, MI, May 1-3, 2000.

The research described in this paper was carried out at the Jet Propulsion Laboratory, California Institute of Technology, under a contract with the National Aeronautics and Space Administration.